Neoplasia • Vol. 3, No. 3, 2001, pp. 189–195

www.nature.com/neo

Using Positron Emission Tomography with [^{18}F]FDG to Predict Tumor Behavior in Experimental Colorectal Cancer[1]

Bryan M. Burt, John L. Humm†, David A. Kooby*, Olivia D. Squire†, Stephen Mastorides‡, Steve M. Larson† and Yuman Fong**

Department of *Surgery, †Nuclear Medicine, ‡Pathology, Memorial Sloan-Kettering Cancer Center, New York, NY 10021

Abstract

This study investigates the relationship between FDG uptake as determined by positron emission tomography (PET) imaging and rates of tumor growth, cellular GLUT1 transporter density, and the activities of hexokinase and glucose-6-phosphatase in a solid tumor implant model. Five different human colorectal xenografts of different growth properties were implanted in athymic rats and evaluated by dynamic ^{18}F-FDG-PET. The phosphorylating and dephosphorylating activities of the key glycolytic enzymes, hexokinase and glucose-6-phosphatase, were measured in these tumor types by spectrophotometric assays and the expression of GLUT1 glucose transporter protein was determined by immunohistochemistry. Correlations among FDG accumulation, hexokinase activity, and tumor doubling time are reported in these colon xenografts. The results indicate that the activity of tumor hexokinase may be a marker of tumor growth rate that can be determined by ^{18}F-FDG-PET imaging. PET scanning may not only be a useful tool for staging patients for extent of disease, but may provide important prognostic information concerning the proliferative rates of malignancies. *Neoplasia* (2001) **3,** 189–195.

Keywords: FDG, GLUT, hexokinase, PET, tumor growth.

Introduction

It has been long noted that neoplastic tissues have increased rates of glycolysis [1]. The increased utilization of glucose by tumors has been attributed to both an increased activity of membrane glucose transporters such as GLUT1 [2–5], as well as an increase in rate-limiting enzymes of the glycolytic pathway including hexokinase [6,7]. This high consumption of glucose provides energy for cell growth and also provides precursors for nucleotide and lipid synthesis [8]. Using a fluorinated glucose analog, [^{18}F]2-fluoro-2-deoxy-D-glucose (FDG), positron emission tomography (PET) exploits these tumor-related cellular changes to provide detection and staging of a variety of human malignancies [9–13]. Like glucose, FDG is transported by GLUT1. After phosphorylation by hexokinase, however, FDG-6-phosphate cannot proceed along the glycolytic pathway because it is not a substrate for the next enzyme in the glycolytic pathway, phosphohexose isomerase. ^{18}F-FDG-6-phosphate is essentially trapped within the tumor cell and may be imaged by PET. This imaging technique has moved into the clinical realm of diagnosis, staging, and treatment planning [9,14,15].

Indirect evidence suggests that FDG accumulation may reflect tumor aggressiveness. There is correlation between the accumulation of FDG and histological grade in lung, brain, hepatic, and musculoskeletal neoplasms [9,10,17–19]. Correlations among tumor FDG accumulation, cell cycle, Ki-67 indices, and p53 overexpression have also been reported [16,17,20–22]. This report extends these previous observations by comparison of ^{18}F-FDG-PET findings with the growth rates of colorectal tumor implants in an animal xenograft model and evaluates the biochemical determinants of FDG uptake.

Materials and Methods

Animals and Tumors

Tumor cells. Five colorectal carcinoma cell lines were used in this study. HCT8, HT29, and LS174T were obtained from the American Type Culture Collection (Rockville, MD). C29 and C85 were isolated and characterized at Memorial Sloan-Kettering Cancer Center as previously described [23]. C85, C29, and HCT8 were cultured in RPMI with 10% fetal calf serum (FCS) supplemented with 5 mM L-glutamine. LS174T was cultured in RPMI with 10% FCS and non-essential amino acids and 5 mM L-glutamine. HT29 was cultured in McCoy's 5A media with 10% FCS. Cells were maintained in a 5% CO_2 humidified environment at 37°C. Histologically, these cell lines produce tumors that range from moderate grade (C29, HCT8, and HT29) to moderate/poor grade (C85 and LS174T) [23].

Abbreviations: FDG, [^{18}F]fluorodeoxyglucose; PET, positron emission tomography

Address all correspondence to: Yuman Fong, Department of Surgery, Memorial Sloan-Kettering Cancer Center, 1275 York Avenue, New York, NY 10021. E-mail: fongy@mskcc.org

[1]This work was supported, in part, by United States Public Health Service grants RO1CA75416, RO1CA72632, and RO1CA61524 from the National Institutes of Health and MBC-99366 from the American Cancer Society.

Received 4 December 2000; Accepted 10 January 2001.

Animal models All experiments were performed under guidelines approved by the Memorial Sloan-Kettering Institutional Animal Care and Use Committee. Male athymic rats (National Cancer Institute, Bethesda, MD) were used in all animal studies. Five human colorectal cancer cell lines were used to establish xenografts at two or three sites at the base of the neck on the anterior chest wall. This site was selected in order to avoid body areas with high FDG uptake such as the brain, heart, and bladder. Tumor cells (2×10^6 in 50 μl of culture media) were injected subcutaneously at each tumor site. In any individual animal, all xenografts were derived from the same cell line. Tumor volumes were calculated three times per week using the formula for a prolate spheroid, $4/3(\pi)ab^2$, with a as the radius of the long axis and b as the radius of the short axis in millimeters [23]. These measurements were carefully performed with vernier calipers. The $\log_{10}$ of the average tumor volume was plotted against time and tumor doubling time was determined from the logarithmic growth phase.

PET

Rats were imaged by PET when tumor volume reached 350 mm^3 (9.5±1.3 mm diameter) to minimize variations due to partial volume effect. Region of interest (ROI) analyses on tumors of these volumes produce reliable measurements of FDG uptake in experimental models [24]. Five groups of animals were used, with animals bearing xenografts from one of the five cell lines ($n\geq6$ per group). Food was removed from the rats 6 hours prior to injection with FDG and rats weighed approximately 250 g at the time of scan. The PET scan was performed on a clinical GE Advance PET scanner (General Electric, Milwaukee, WI) [25]. Animals were anesthesized with a single intraperitoneal injection of pentobarbital (50 mg/kg) and placed in the supine position on the detector ring. The extremities were extended and restrained by laboratory tape to a Styrofoam platform. FDG, 3.7 MBq (100 μCi), was administered through the tail vein. Dynamic scans were acquired within ten 2-minute frames (from 0 to 20 minutes) and four 5-minute frames (from 20 to 40 minutes), initiated at the time of injection of the radiotracer. A 6-minute transmission scan was performed using two Ge-68 rods immediately upon completion of the dynamic scan. Images were reconstructed using attenuation correction by filtered back projection into a (128×128) matrix by a Hanning filter with an 8.5-mm cutoff frequency and 4-mm Gaussian smoothing in three dimensions.

ROIs were drawn according to the methodology of Erdi *et al.* [26]. In brief, this is an adaptive thresholding technique in which regions are manually drawn around the lesion circumference, but at specific window display setting on the PET workstation, corresponding to the appropriate lesion size and contrast. ROIs were drawn around each of the tumors in the frame for which the tumor showed maximum radioactivity. Serial changes of maximum tumor radioactivity (nCi/ml tissue) were determined dynamically from a sequence of images. Standard uptake value (SUV) analysis was performed for each tumor from the images acquired following FDG administration. SUV is defined as the tumor tissue activity (μCi/ml) divided by the injected dose (μCi) per body weight of the rat (g). The maximum SUV utilizes the activity per milliliter in the hottest pixel within a ROI delineating the tumor and yields the highest measured SUV for the tumor. All SUVs were obtained from the final 5-minute frame, when tumor uptake had reached a plateau. Recovery coefficients for the GE Advance were measured using spheres of several different diameters (4 to 27 mm) containing known specific activities of F-18 within a cylindrical Jaszczak phantom. The entire SUV data were then corrected for partial volume effects by dividing the specific activity determined for every tumor ROI with the recovery coefficient for a sphere of the same equivalent diameter. The SUV is then given by this partial volume effect corrected lesion activity per gram divided by the quotient of the injected activity and the rat weight. In all tumors, FDG uptake was lower than the liver, brain, heart, and bladder, and for this reason, the tumors were grown on the anterior chest wall at the base of the neck to provide adequate contrast for visualization.

Tissue Excision and Analysis

Separate groups of four to six animals per tumor type were used to characterize the xenograft enzyme activities (n=6), GLUT1 glucose transporter expression (n=4), and tumor growth rates ($n\geq6$). When tumor volume reached 350 mm^3, animals were sacrificed by CO_2 inhalation. Tissues were excised and immediately assayed for hexokinase and glucose-6-phosphatase or fixed in paraformaldehyde for immunohistochemical analysis of paraffin sections.

Enzyme assays Hexokinase (EC 2.7.1.1) and glucose-6-phosphatase (EC 3.1.3.9) activities were measured in accordance with the methods of Bergmeyer [27]. Upon sacrifice, tumors were removed, washed in phosphate-buffered saline (PBS), and cut into halves. One portion was used for determination of hexokinase and the other portion for determination of glucose-6-phosphatase.

Hexokinase was determined spectrophotometrically by measuring the reduction rate of nicotinamide adenine dinucleotide phosphate at 340 nm with glucose-6-phosphate dehydrogenase. Tissues were homogenized in 4 vol of buffer containing 150 mM KCl, 5 mM $MgCl_2$, 5 mM EDTA, and 5 mM 2-mercaptoethanol. The high-speed supernatant (100,000g for 30 minutes) was assayed. The reaction cocktail consisted of 40 mM triethanolamine buffer (pH 7.6), 8 mM $MgCl_2$, 0.91 mM β-NADP, 0.64 mM ATP, 1.5 U glucose-6-phosphate dehydrogenase, and 5 mM glucose. One unit of hexokinase activity catalyzed the formation of 1 nmol of glucose-6-phosphate per minute in the presence of 5 mM glucose. Activities are expressed as units per milligram protein.

For determination of glucose-6-phosphatase, tissues were homogenized in 4 vol of a 0.25 M sucrose solution. Pure tissue homogenates were assayed to determine the amount of inorganic phosphate liberated per unit time by the formation of a blue phosphomolybdous complex that is visible at 700 nm. One unit of activity corresponded to the formation of 1 nmol of inorganic phosphate liberated per minute. Enzyme activities were standardized to total protein content determined according to the methods of Bradford [28].

Immunohistochemistry

GLUT1 The polyclonal rabbit antiglucose transporter protein reactive with GLUT-1 (rat) (Alpha Diagnostic, San Antonio, TX) was raised against synthetic peptide (12-mer) based on the deduced amino acid sequence of the carboxy terminus of the rat brain glucose transporter. This antibody immunoreacts with human and rat tissues expressing the GLUT1 protein. It was diluted 1:20,000 with PBS (PBS) containing 2% bovine serum albumin (Sigma, St. Louis, MO). The bound antibody was visualized by routine avidin/biotin conjugate immunoperoxidase procedure using the Vectastain Elite kit (Vector, Burlingame, CA) [29].

Paraffin sections (8 μm thick) were deparaffinized with histoclear and an ethanol gradient. Sections were washed in PBS and then quenched in 10% hydrogen peroxide (Sigma). Antigen retrieval was performed in 0.01 M citric acid (pH 6) for 15 minutes at high power in a laboratory microwave. Sections were washed in PBS and then blocked with avidin, biotin, and then 10% normal goat serum. Sections were again washed in PBS and then incubated overnight with the primary antibody at 4°C. Finally, peroxidase activity was demonstrated using 3,3′-diaminobenzidine tetrahydrochloride (DAB) (Sigma) as substrate–chromogen solution. Sections were lightly counterstained with Harris hematoxylin, dehydrated in graded ethanol and then histoclear, and mounted.

To confirm specificity of GLUT1 staining, parallel sections were stained with GLUT1 antiserum that had been previously incubated with excess of immunizing peptide antigen (50 μg/ml). Sections of paraffin-embedded 7.5-day-old mouse embryos and mouse testis were used as positive controls.

Immunohistochemical grading The immunoreactivity of GLUT1 was evaluated by one pathologist blinded to tumor growth rate, SUV, and enzyme activities. GLUT1 immunostaining was quantitated by grading the proportion of viable cancer cells that were GLUT1-positive [30]. Sections with cancer cells that positively demonstrated membranous staining at any frequency and intensity were considered GLUT-positive.

Statistical Analysis

Differences among groups of measurements were analyzed using a Student's *t*-test. A *P* value of .05 or less was considered significant. Least-squares linear regressions were used to analyze relationships among SUV, hexokinase activity, and tumor doubling time.

Results

PET

Dynamic PET images were obtained for each animal. The site of tumor implantation was chosen to ensure that each tumor was readily distinguished from the surrounding tissues. Figure 1*A* and *B* are representative PET images of C85 and C29 xenograft-bearing rats obtained during the 40th minute of the scan. Figure 2 shows the mean tissue time–activity curves for each xenograft. The rate of accumulation of FDG in all tumors demonstrated a plateau. By 40 minutes, LS174T xenografts demonstrated the highest FDG uptake (667±4 nCi/ml tissue, SUV 2.20±0.16) and the C29 xenograft showed the lowest uptake (259±18 nCi/ml, SUV 1.27±0.21). HCT8, C85, and HT29 showed moderate uptake of FDG (447±36, 487±32, 457±66 nCi/ml; SUV 1.74±0.22, 1.84±0.26, 1.57±0.34). These data are shown in Figure 2 as maximum SUV of each xenograft plotted against time and in Figure 3 as maximum SUV calculated at 40 minutes for each xenograft. At 40 minutes, SUV measurements varied significantly ($P<.05$) among xenografts of the various cell lines.

Enzyme Analysis

A summary of enzyme data is provided in Table 1. Hexokinase activities varied significantly among tumor types (Table 1). LS174T xenografts demonstrated the highest hexokinase activities (25.3±5.6); HCT8, C85, and HT29 xenografts demonstrated moderate activities (20.4±3.4, 23.3±2.0, 23.4±6.5); and C29 xenografts demonstrated the lowest activities (13.3±1.7). A direct correlation between SUV and levels of hexokinase was found in these five colorectal xenografts ($r=0.9$; Figure 4). No statistical differences in glucose-6-phosphatase activities were apparent among these colon tumors (Table 1).

Doubling Time

In vivo tumor volume doubling times ranged from 45 hours (LS174T) to 184 hours (C29). SUV correlated directly with *in vivo* tumor doubling time ($r=0.82$; Figure 5). Hexokinase activity in tumor tissues also correlated with *in vivo* tumor doubling time ($r=0.83$; Figure 5).

Immunohistochemistry

All xenografts showed specific GLUT1 immunostaining of the plasma membrane in at least 10% of viable cancer cells. Expression of GLUT1 varied from moderate to intense and was especially prominent at cell–cell boundaries. In all cases, this reticulated GLUT1 staining pattern was abolished by preincubation of the antiserum with GLUT1 peptide. The highest levels of GLUT1 expression were observed in clusters of cells within glandular units and in cell layers bordering necrotic islands. The frequency of GLUT1 immu-

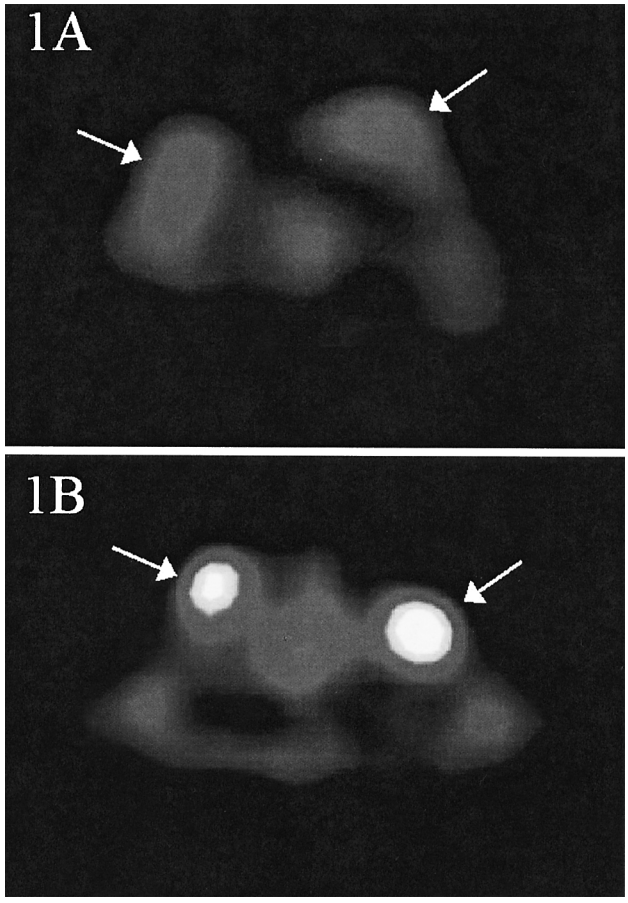

Figure 1. *Cross-sectional PET images of tumor-bearing rats taken 40 minutes following intravenous administration of FDG. Rats are in the supine position and the level of cross section is at the upper thorax. Xenografts (arrows) are located on the superior anterior chest wall at the base of the neck. Areas of brightness represent regions of greater [^{18}F]FDG concentration. (A) Rat bearing two representative C85 human colorectal xenografts. (B) Rat bearing two representative C29 human colorectal xenografts.*

nostaining was consistent among sections from tumors of the same cell line and among different sections of the same tumor within variation of less than 10%. The results for GLUT1 expression are summarized in Table 1. Sections from HT29 and HCT8 xenografts stained positively for

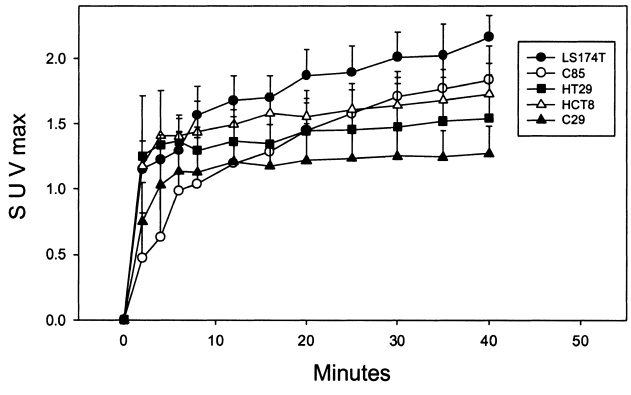

Figure 2. *Average time–activity curves of [^{18}F]FDG accumulation in five human colorectal xenografts. Data points represent then mean (±SD) for each set of xenografts.*

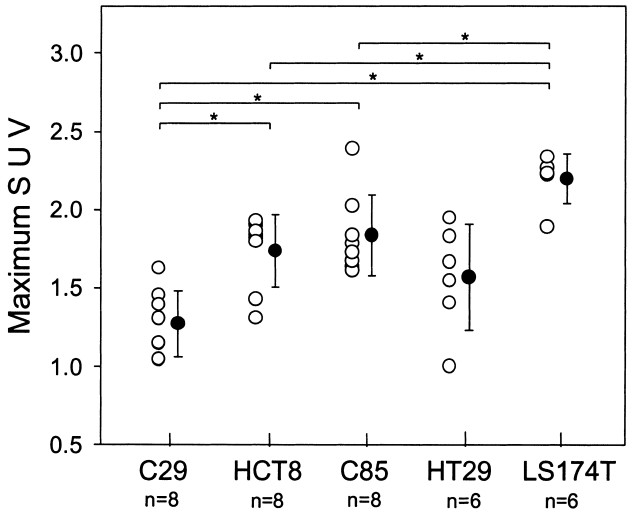

Figure 3. *Comparison of maximum SUVs of five human colorectal xenografts. Open circles represent individual SUV values and closed circles represent the mean (±SD) for each set of values. Significance differences between groups of xenografts is indicated by (*).*

GLUT1 at a greater frequency (40% to 80%) than sections from C29, C85, and LS174T xenografts (10%). There was no apparent correlation of GLUT1 to either doubling time or SUV.

Discussion

PET after administration of the glucose analogue, [^{18}F]fluorodeoxyglucose, is a non-invasive imaging modality that has substantial potential for managing patients with cancer. This imaging modality exploits the high glucose utilization of tumor cells for imaging of metastases [31]. For glucose-avid tumors such as colorectal neoplasms, there is sufficient evidence that FDG-PET may assist in detection of occult disease and FDG-PET is currently utilized clinically for improved staging of patients [32–34]. Unlike other imaging modalities, PET supplies a quantitative metabolic characterization of tissues that may also provide information concerning tumor behavior. The current experiments were therefore designed to test the hypothesis that FDG-PET characteristics correlate with tumor proliferative rates and rate-limiting glycolytic enzyme activity. Using a series of cell lines with diverse growth rates, results of dynamic ^{18}F-FDG-PET scanning confirm that tumors may reach characteristic plateau FDG uptakes that correlate with growth.

FDG studies have been performed on transformed and malignant tissues *in vitro* to elucidate the mechanisms of increased tumor glucose utilization, and yet no consensus has been reached as to which element in cellular metabolism is most important for cellular retention and uptake of FDG [35–38]. Three main factors are thought to be the most influential on cellular FDG accumulation. FDG is transported into the cell by glucose transport proteins such as GLUT1 [39]. Once transported into the cell, FDG is phosphorylated by the glycolytic enzyme hexokinase to become ^{18}F-FDG-PO_4, which is selectively retained within the tumor cell because of the low membrane permeability of FDG-6-

Table 1. Glycolytic Parameters, Tumor Doubling Times, and SUV_{max} for Five Human Colorectal Cancer Xenografts.

Xenograft	Hexokinase (U/mg)*	G-6-PASE (U/mg)*	GLUT1 (%)†	Doubling Time (hours)	SUV_{max}‡
C29	13.3±1.7	30.9±1.9	10	184	1.27±0.21 (n=8)
HCT8	20.4±3.4§,¶	29.9±1.7	80	173	1.74±0.22§,¶ (n=8)
C85	23.3±2.0§	29.5±2.1	10	120	1.84±0.26§,¶ (n=8)
HT29	23.4±6.5§	28.7±1.9	40	110	1.57±0.34§ (n=6)
LS174T	25.3±5.6§	42.7±10.8	10	45	2.20±0.16§ (n=6)

Data are presented as mean±SD.
*Activity of hexokinase and glucose-6-phosphatase was measured as described in the Materials and Methods section.
†Each value represents the relative percentage of GLUT1-positive cells per section of tissue.
‡Maximum SUV value is the activity per milliliter in the hottest pixel within a ROI delineating the tumor. It is the highest measured SUV for the tumor.
§Differences between each HCT8, C85, and LS174T xenograft and C29 xenograft were significant (P<.05).
¶Differences between each HCT8 and C85 xenograft and LS174T xenograft were significant (P<.05).

phosphate [40]. The levels of FDG-PO_4 also depend on the activity of glucose-6-phosphatase, the enzyme which removes the phosphate from this compound. The current report demonstrates that tumor cell hexokinase is more important than glucose-6-phosphatase activity or GLUT1-mediated transport in influencing the accumulation of FDG in this *in vivo* rat xenograft model. Furthermore, this FDG accumulation as imaged by whole-body PET can be used to assess tumor growth rate.

The idea that cellular glucose metabolism may correlate to tumor growth and aggressiveness has been suggested in past studies. Previous reports have demonstrated a correlation of glucose metabolism with tumor growth rate and with the loss of histological differentiation in transplantable rat tumors [41,42]. In addition, the glucose transporter protein GLUT1 has been documented to be expressed in high levels in tumor cells [30,43]. Glucose transporter protein expression is also rapidly induced experimentally by growth factors such as fibroblast growth factor, platelet-derived growth factor, or epidermal growth factor [44]. These same factors have been demonstrated to be local growth factors, trophic for colorectal cancer growth, and tumor levels of these growth factors have been found to be prognostic for outcome [45,46]. In breast cancer, GLUT1 expression has been correlated to higher grade and proliferative rate of tumors [43]. In lung cancer, GLUT1 and GLUT3 expression has been associated with poor survival [30]. Glucose transporter protein expression may therefore be a marker and a cause of increased tumor aggressiveness. Although faint expression of a number of the seven identified GLUT transporters may be observed, it has been established that GLUT1 is the most highly expressed in colon cancers [5] and small cell lung carcinoma [47]. In the current *in vivo* studies, we did not find a correlation of GLUT1 expression to either tumor growth rates or to FDG accumulation. Whether other less commonly expressed GLUTs contribute to FDG transport in this model was not specifically addressed here. In the tumors examined, hexokinase activity appears to be a more important determinant of cellular glucose and FDG metabolism. Whether in tumors of equal hexokinase activity the GLUT1 expression will distinguish tumors in terms of behavior cannot be determined from the limited number of tumors assayed.

In normal tissues, significant glucose-6-phosphatase activity has been shown to correlate with the rapid clearance

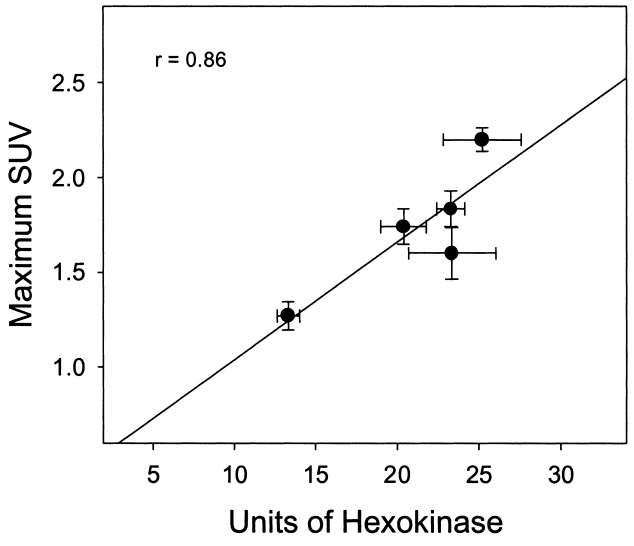

Figure 4. *Correlation of maximum SUV (mean±SEM) with the activity of hexokinase (mean±SEM) in five human colorectal xenografts. Each xenograft is represented by a filled circle.*

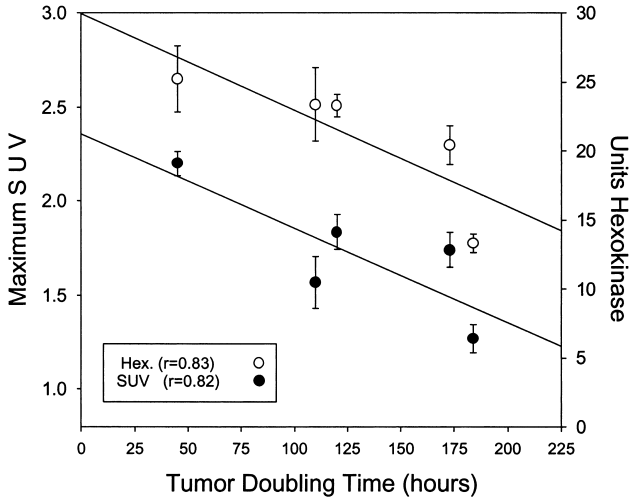

Figure 5. *The relationship between tumor doubling time, maximum SUV, and hexokinase. SUV_{max} (mean±SEM) for each colorectal xenograft (open circles), and the activity of hexokinase (mean±SEM) for each colorectal xenograft (filled circles) are both correlated to the tumor doubling time.*

of titrated deoxyglucose [35]. Unlike tissues such as liver or kidney, glucose-6-phosphatase levels have been found at low levels in tumors [48,49]. The current study confirmed the low level of glucose-6-phosphatase activity in colorectal cancer cells, and found that such activity was not significantly different among the various colon tumors. These data suggest that neither GLUT1 or glucose-6-phosphatase in colon tumors plays a rate-limiting role *in vivo* in regulating the accumulation of FDG in these cell lines in a rat xenograft model.

Rather, hexokinase activity demonstrated the greatest correlation with FDG and tumor behavior in this xenograft model of colorectal cancer. Hexokinase begins the first step of the glycolytic cycle and is overexpressed in many tumors [6,7,50–53]. In fact, of the four hexokinase isozymes (I, II, III, and IV), it appears that type II isoenzymes, and to a lesser degree type I, are overexpressed in highly glycolytic, rapidly growing tumors [31]. Concentration of FDG-6-phosphate in liver and esophageal malignancies has been shown to correlate with tissue levels of hexokinase [9,11]. The current study extends these observations in documenting not only that FDG imaging is most dependent on cellular hexokinase levels, but that the hexokinase activity and FDG accumulation as imaged by PET reflect tumor proliferative rates.

Some clinical observations are consistent with our current findings. Glucose metabolic rates as determined by ^{18}F-FDG PET have been found to parallel changes in tumor size on repeated computed tomography scans in four patients with intracranial meningioma [54]. FDG uptake has been correlated to pathologic grade in a large array of human malignancies [9,16–20]. There have also been descriptions of changes in ^{18}F-FDG uptake correlating to change in tumor histology. In the treatment of testicular cancers with chemotherapy, there is often a change in histologic appearance of the tumor from the more poorly differentiated embryonal carcinoma to the more well-differentiated mature teratoma. Such a shift in histology has been seen coincident with a decrease in FDG uptake by PET scanning [55]. Similarly, FDG-PET imaging with FDG corresponds with histological response to chemotherapy and survival in breast cancer [56,57].

We have been cautious in our interpretation of the current data because of certain obvious limitations. Firstly, though tumor cell lines and xenografts are well accepted and important experimental model systems, they clearly do not mimic natural tumors exactly. For example, the doubling times for tumor cells lines in culture and used to produce xenograft models exhibit much greater doubling times than natural human malignancies. Also, there are significant differences in the stromal bed and blood supply. It has been previously noted and has been confirmed in the current experiment that the SUVs are much lower in tumor xenograft models than in cancers seen in patients. Nevertheless, tumor cell lines and xenografts are invaluable in the study of biology of tumors. Furthermore, tumor blood flow measurements were not performed in this study and therefore, the contribution of varying blood flow in different tumor types to tumor FDG accumulation cannot be determined.

Our study is an experimental confirmation of a correlation between FDG metabolism and tumor proliferative rates and suggests that the FDG-PET may be useful in determination of tumor prognosis and possibly even sensitivity to adjuvant therapies. This imaging modality may accomplish such assessment in a non-invasive manner. These preclinical data, along with the preliminary clinical observation available, strongly encourage clinical trials in diverse tumor types examining the prognostic significance of tumor FDG accumulation as imaged by whole-body PET scanning.

Acknowledgements

The authors thank Yong-Jia You for excellent technical support and Katia Manova and Karen Witty-Blease for expert assistance with immunohistochemical staining and analysis.

References

[1] Warburg O (1956). On the origin of cancer cells. *Science* **123**, 309–314.

[2] Younes M, Lechago LV, Somoano JR, Mosharaf M, and Lechago J (1996). Wide expression of the human erythrocyte glucose transporter Glut1 in human cancers. *Cancer Res* **56**, 1164–1167.

[3] Brown RS, Leung JY, Fisher SJ, Frey KA, Ethier SP, and Wahl RL (1996). Intratumoral distribution of tritiated FDG in breast carcinoma: correlation between Glut-1 expression and FDG uptake. *J Nucl Med* **37**, 1042–1047.

[4] Higashi T, Tamaki N, Torizuka T, Nakamoto Y, Sakahara H, Kimura T, Honda T, Inokuma T, Katsushima S, Ohshio G, Imamura M, and Konishi J. (1998). FDG uptake, GLUT-1 glucose transporter and cellularity in human pancreatic tumors. *J Nucl Med* **39**, 1727–1735.

[5] Chung JK, Lee YJ, Kim C, Choi SR, Kim M, Lee K, Jeong JM, Lee DS, Jang JJ, and Lee MC (1999). Mechanisms related to [^{18}F]fluorodeoxyglucose uptake of human colon cancers transplanted in nude mice. *J Nucl Med* **40**, 339–346.

[6] Rempel A, Bannasch P, and Mayer D (1994). Differences in expression and intracellular distribution of hexokinase isoenzymes in rat liver cells of different transformation stages. *Biochim Biophys Acta* **1219**, 660–668.

[7] Mathupala SP, Rempel A, and Pedersen PL (1995). Glucose catabolism in cancer cells. Isolation, sequence, and activity of the promoter for type II hexokinase. *J Biol Chem* **270**, 16918–16925.

[8] Weber G (1977). Enzymology of cancer cells (second of two parts). *N Engl J Med* **296**, 541–551.

[9] Okazumi S, Isono K, Enomoto K, Kikuchi T, Ozaki M, Yamamoto H, Hayashi H, Asano T, and Ryu M (1992). Evaluation of liver tumors using fluorine-18-fluorodeoxyglucose PET: characterization of tumor and assessment of effect of treatment [see comments]. *J Nucl Med* **33**, 333–339.

[10] Mankoff DA, Dehdashti F, and Shields AF (2000). Characterizing tumors using metabolic imaging: PET imaging of cellular proliferation and steroid receptors. *Neoplasia* **2**, 71–88.

[11] Fukunaga T, Okazumi S, Koide Y, Isono K, and Imazeki K (1998). Evaluation of esophageal cancers using fluorine-18-fluorodeoxyglucose PET. *J Nucl Med* **39**, 1002–1007.

[12] Minn H, Lapela M, Klemi PJ, Grenman R, Leskinen S, Lindholm P, Bergman J, Eronen E, Haaparanta M, and Joensuu H (1997). Prediction of survival with fluorine-18-fluoro-deoxyglucose and PET in head and neck cancer. *J Nucl Med* **38**, 1907–1911.

[13] Wahl RL, Cody RL, Hutchins GD, and Mudgett EE (1991). Primary and metastatic breast carcinoma: initial clinical evaluation with PET with the radiolabeled glucose analogue 2-[F-18]-fluoro-2-deoxy-D-glucose. *Radiology* **179**, 765–770.

[14] Fong Y, Saldinger PF, Akhurst T, Macapinlac H, Yeung H, Finn RD, Cohen A, Kemeny N, Blumgart LH, and Larson S (1999). Utility of 18F-FDG-PET scanning on selection of patients for resection of hepatic colorectal metastases. *Am J Surg* **178**, 282–287.

[15] Ito K, Kato T, Tadokoro M, Ishiguchi T, Oshima M, Ishigaki T, and

Sakuma S (1992). Recurrent rectal cancer and scar: differentiation with PET and MR imaging. *Radiology* **182**, 549–552.
[16] Vesselle H, Schmidt RA, Pugsley JM, Li M, Kohlmyer SG, Vallires E, and Wood DE (2000). Lung cancer proliferation correlates with [F-18]fluorodeoxyglucose uptake by positron emission tomography [in process citation]. *Clin Cancer Res* **6**, 3837–3844.
[17] Folpe AL, Lyles RH, Sprouse JT, Conrad EU III, and Eary JF (2000). (F-18)fluorodeoxyglucose positron emission tomography as a predictor of pathologic grade and other prognostic variables in bone and soft tissue sarcoma. *Clin Cancer Res* **6**, 1279–1287.
[18] Kaschten B, Stevenaert A, Sadzot B, Deprez M, Degueldre C, Del Fiore G, Luxen A, and Reznik M (1998). Preoperative evaluation of 54 gliomas by PET with fluorine-18-fluorodeoxyglucose and/or carbon-11-methionine. *J Nucl Med* **39**, 778–785.
[19] Kern KA, Brunetti A, Norton JA, Chang AE, Malawer M, Lack E, Finn RD, Rosenberg SA, and Larson SM (1988). Metabolic imaging of human extremity musculoskeletal tumors by PET. *J Nucl Med* **29**, 181–186.
[20] Okada J, Yoshikawa K, Itami M, Imaseki K, Uno K, Itami J, Kuyama J, Mikata A, and Arimizu N (1992). Positron emission tomography using fluorine-18-fluorodeoxyglucose in malignant lymphoma: a comparison with proliferative activity. *J Nucl Med* **33**, 325–329.
[21] Lippitz B, Cremerius U, Mayfrank L, Bertalanffy H, Raoofi R, Weis J, Bocking A, Bull U, and Gilsbach JM (1996). PET study of intracranial meningiomas: correlation with histopathology, cellularity and proliferation rate. *Acta Neurochir Suppl (Wien)* **65**, 108–111.
[22] Minn H, Joensuu H, Ahonen A, and Klemi P (1988). Fluorodeoxyglucose imaging: a method to assess the proliferative activity of human cancer *in vivo*. Comparison with DNA flow cytometry in head and neck tumors. *Cancer* **61**, 1776–1781.
[23] Kooby DA, Carew JF, Halterman MW, Mack JE, Bertino JR, Blumgart LH, Federoff HJ, and Fong Y (1999). Oncolytic viral therapy for human colorectal cancer and liver metastases using a multimutated herpes simplex virus type-I (G207). *FASEB J* **13**, 1325–1334.
[24] Humm J, Lee J, O'Donoghue J, Squire O, Ling C, Pentlow K, Erdi Y, Mehta B, Ruan S, and Larson S (1999). Changes in FDG tumor uptake during and after radiation therapy in a rodent tumor xenograft. *J Clin Positron Imaging* **2**, 289–296.
[25] DeGrado TR, Turkington TG, Williams JJ, Stearns CW, Hoffman JM, and Coleman RE. (1994). Performance characteristics of a whole-body PET scanner. *J Nucl Med* **35**, 1398–1406.
[26] Erdi YE, Mawlawi O, Larson SM, Imbriaco M, Yeung H, Finn R, and Humm JL. (1997). Segmentation of lung lesion volume by adaptive positron emission tomography image thresholding. *Cancer* **80**, 2505–2509.
[27] Bergmeyer HU (1974). *Methods of Enzymatic Analysis* (Vol. 1). Academic Press, New York.
[28] Bradford MM (1976). A rapid and sensitive method for the quantitation of microgram quantities of protein utilizing the principle of protein-dye binding. *Anal Biochem* **72**, 248–254.
[29] Hsu SM, Raine L, and Fanger H (1981). Use of avidin-biotin-peroxidase complex (ABC) in immunoperoxidase techniques: a comparison between ABC and unlabeled antibody (PAP) procedures. *J Histochem Cytochem* **29**, 577–580.
[30] Younes M, Brown RW, Stephenson M, Gondo M, and Cagle PT (1997). Overexpression of GLUT1 and GLUT3 in stage 1 non-small cell lung carcinoma is associated with poor survival. *Cancer* **80**, 1046–1051.
[31] Rempel A, Mathupala SP, Griffin CA, Hawkins AL, and Pedersen PL (1996). Glucose catabolism in cancer cells: amplification of the gene encoding type II hexokinase. *Cancer Res* **56**, 2468–2471.
[32] Beets G, Penninckx F, Schiepers C, Filez L, Mortelmans L, Kerremans R, Aerts R, and De Roo M (1994). Clinical value of whole-body positron emission tomography with [^{18}F]fluorodeoxyglucose in recurrent colorectal cancer. *Br J Surg* **81**, 1666–1670.
[33] Vitola JV, Delbeke D, Sandler MP, Campbell MG, Powers TA, Wright JK, Chapman WC, and Pinson CW (1996). Positron emission tomography to stage suspected metastatic colorectal carcinoma to the liver. *Am J Surg* **171**, 21–26.
[34] Lai DTM, Fulham M, Stephen MS, Chu KM, Solomon M, Thompson JF, Sheldon DM, and Storey DW (1996). The role of whole-body positron emission tomography with [^{18}F]fluorodeoxyglucose in identifying operable colorectal cancer metastases to the liver. *Arch Surg* **131**, 703–707.
[35] Nelson CA, Wang JQ, Leav I, and Crane PD (1996). The interaction among glucose transport, hexokinase, and glucose-6-phosphatase with respect to 3*H*-2-deoxyglucose retention in murine tumor models. *Nucl Med Biol* **23**, 533–541.
[36] Haberkorn U, Ziegler SI, Oberdorfer F, Trojan H, Haag D, Peschke P, Berger MR, Altmann A, and van KG (1994). FDG uptake, tumor proliferation and expression of glycolysis associated genes in animal tumor models. *Nucl Med Biol* **21**, 827–834.
[37] Kim BK, Chung JK, Lee YJ, Jeong JM, Lee DS, and Lee MC (1999). Accumulation with expressions of glucose transporter-1 and hexokinase in human cancer cell lines. *J Nucl Med* **40** (5), 224.
[38] Brown RS, Goodman T, Kison PV, Zasadny KR, and Wahl RL (1999). Variable expression of Glut-1 and hexokinase in human breast and lung cancer. *J Nucl Med* **40** (5), 22.
[39] Kahn BB, and Flier JS (1990). Regulation of glucose-transporter gene expression *in vitro* and *in vivo*. *Diabetes Care* **13**, 548–564.
[40] Aloj L, Caraco C, Jagoda E, Eckelman WC, and Neumann RD (1999). Glut-1 and hexokinase expression: relationship with 2-fluoro-2-deoxy-D-glucose uptake in A431 and T47D cells in culture. *Cancer Res* **59**, 4709–4714.
[41] Knox WE, Jamdar SC, and Davis PA (1970). Hexokinase, differentiation and growth rates of transplanted rat tumors. *Cancer Res* **30**, 2240–2244.
[42] Sweeney MJ, Ashmore J, Morris HP, and Weber G (1963). Comparative biochemistry of hepatomas: IV. Isotope studies of glucose and fructose metabolism in liver tumors of different growth rates. *Cancer Res* **23**, 995–1002.
[43] Younes M, Brown RW, Mody DR, Fernandez L, and Laucirica R (1995). GLUT1 expression in human breast carcinoma: correlation with known prognostic markers. *Anticancer Res* **15**, 2895–2898.
[44] Hiraki Y, Rosen OM, and Birnbaum MJ (1988). Growth factors rapidly induce expression of the glucose transporter gene. *J Biol Chem* **263**, 13655–13662.
[45] Friedman E, Gold LI, Klimstra D, Zeng ZS, Winawer S, and Cohen A (1995). High levels of transforming growth factor beta 1 correlate with disease progression in human colon cancer. *Cancer Epidemiol, Biomarkers Prev* **4**, 549–554.
[46] Hsu S, Huang F, Hafez M, Winawer S, and Friedman E (1994). Colon carcinoma cells switch their response to transforming growth factor beta 1 with tumor progression. *Cell Growth Differ* **5**, 267–275.
[47] Brown RS, Leung JY, Kison PV, Zasadny KR, Flint A, and Wahl RL (1999). Glucose transporters and FDG uptake in untreated primary human non-small cell lung cancer. *J Nucl Med* **40**, 556–565.
[48] Weber G, and Cantero A (1963). Glucose-6-phosphatase activity in normal, precancerous, and neoplastic tissues. *Cancer Res* **15**, 105–108.
[49] Weber G, and Morris H (1963). Comparative biochemistry of hepatomas: III. Carbohydrate enzymes in liver tumors of different growth rates. *Cancer Res* **23**, 987–994.
[50] Rempel A, Bannasch P, and Mayer D (1994). Differences in expression and intracellular distribution of hexokinase isoenzymes in rat liver cells of different transformation. *Biochim Biophys Acta* **1219**, 660–668.
[51] Kikuchi Y, Sato T, and Sugimura T (1972). Hexokinase isoenzyme patterns of human uterine tumors. *Cancer* **30**, 444–447.
[52] Nakashima R, Paggi MG, Scott LJ, and Pedersen PL (1988). Purification and characterization of a bindable form of mitochondrial bound hexokinase from the highly glycolytic AS-30D rat hepatoma cell line. *Cancer Res* **48**, 913–919.
[53] Thelen TA, and Wilson JE (1991). Complete amino acid sequences of the type II isozyme of rat hexokinase, deduced from the cloned cDNA: comparison with a hexokinase from Novikoff ascites tumor. *Arch Biochem Biophys* **286**, 645–651.
[54] Di Chiro G, Hatazawa J, Katz DA, Rizzoli HV, and De Michele DJ (1987). Glucose utilization by intracranial meningiomas as an index of tumor aggressivity and probability of recurrence: a PET study. *Radiology* **164**, 521–526.
[55] Reinhardt MJ, Muller-Mattheis VGO, Gerharz CD, Vosberg HR, Ackermann R, and Muller-Gartner H-W (1997). FDG-PET evaluation of retroperitoneal metastases of testicular cancer before and after chemotherapy. *J Nucl Med* **38**, 99–101.
[56] Smith IC, Welch AE, Hutcheon AW, Miller ID, Payne S, Chilcott F, Waikar S, Whitaker T, Ah-See AK, Eremin O, Heys SD, Gilbert FJ, and Sharp PF (2000). Positron emission tomography using [(18)F]-fluorodeoxy-D-glucose to predict the pathologic response of breast cancer to primary chemotherapy. *J Clin Oncol* **18**, 1676–1688.
[57] Oshida M, Uno K, Suzuki M, Nagashima T, Hashimoto H, Yagata H, Shishikura T, Imazeki K, and Nakajima N (1998). Predicting the prognoses of breast carcinoma patients with positron emission tomography using 2-deoxy-2-fluoro[^{18}F]-D-glucose. *Cancer* **82**, 2227–2234.